Measuring supersymmetric particle masses at the LHC in scenarios with Baryon-number R-parity violating couplings

Ben C. Allanach

Theory Division, CERN, 1211 Geneva 23, Switzerland
E-mail: benjamin.allanach@cern.ch

Alan J. Barr, Lee Drage, Christopher G. Lester, Debbie Morgan
M. Andy Parker, Bryan R. Webber

Cavendish Laboratory, University of Cambridge
Madingley Road, Cambridge, CB3 0HE, UK
E-mail: barr@hep.phy.cam.ac.uk, drage@hep.phy.cam.ac.uk,
lester@hep.phy.cam.ac.uk, morgan@hep.phy.cam.ac.uk,
parker@hep.phy.cam.ac.uk, webber@hep.phy.cam.ac.uk

Peter Richardson

Dept. of Applied Mathematics and Theoretical Physics and Cavendish Laboratory
University of Cambridge, Wilberforce Road, Cambridge, CB3 0WA, UK
E-mail: richardn@hep.phy.cam.ac.uk

ABSTRACT: The measurement of sparticle masses in the Minimal Supersymmetric Standard Model at the LHC is analysed, in the scenario where the lightest neutralino, the $\tilde{\chi}_1^0$, decays into three quarks. Such decays, occurring through the baryon-number violating coupling λ''_{ijk}, pose a severe challenge to the capability of the LHC detectors since the final state has no missing energy signature and a high jet multiplicity. We focus on the case $\lambda''_{212} \neq 0$ which is the most difficult experimentally. The proposed method is valid over a wide range of SUGRA parameter space with $\lambda''_{212} \sim 10^{-5} - 0.1$. Simulations are performed of the ATLAS detector at the Large Hadron Collider. Using the $\tilde{\chi}_1^0$ from the decay chain $\tilde{q}_L \rightarrow \tilde{\chi}_2^0 q \rightarrow \tilde{l}_R \ell q \rightarrow \tilde{\chi}_1^0 \ell \ell q$, we show that the $\tilde{\chi}_1^0$ and $\tilde{\chi}_2^0$ masses can be measured by 3-jet and 3-jet + lepton pair invariant mass combinations. At the SUGRA point $m_0 = 100\,\text{GeV}$, $m_{1/2} = 300\,\text{GeV}$, $A_0 = 300\,\text{GeV}$, $\tan\beta = 10$, $\mu > 0$ and with $\lambda''_{212} = 0.005$, we achieve statistical (systematic) errors of 3 (3), 3 (3), 0.3 (4) and 5 (12) GeV, respectively for the masses of the $\tilde{\chi}_1^0$, $\tilde{\chi}_2^0$, $\tilde{l}_R$ and $\tilde{q}_L$, with an integrated luminosity of $30\,\text{fb}^{-1}$.

KEYWORDS: Supersymmetry Breaking, Supersymmetric Standard Model, Hadronic Colliders.

Contents

1. Introduction

The addition of supersymmetry (SUSY) to the Standard Model (SM) represents a theoretically attractive way of addressing several of the problems faced when attempting to reconcile constraints from fundamental models at high scales with the phenomenology seen at the electroweak scale. In general, supersymmetric models which attempt to solve the naturalness problem, and fix the Higgs mass near the electroweak scale, predict a rich spectrum of physics which can be accessed by experiments at the Large Hadron Collider (LHC). However, most studies of experimental signals for SUSY have assumed that R-parity (R_P) is conserved. R_P is a multiplicative quantum number defined as $(-1)^{3B+L+2S}$ where B and L are baryon and lepton numbers, and S is the spin of the particle. It therefore distinguishes SM particles ($R_P = +1$) from their superpartners ($R_P = -1$).

If R_P is conserved (RPC models), SUSY particles can only be created in pairs, and the lightest SUSY particle (LSP) is stable. Therefore SUSY events each contain an even number of LSPs, which escape detection and give rise to a large missing transverse energy (E_T^{miss}). This signature has been exploited by many analyses of the discovery potential of the LHC [1], since it provides a clean separation between SUSY events and the SM background. However, the incomplete measurement of the final state makes the reconstruction of the SUSY mass spectrum more difficult.

The following terms [2] may be added to the Minimal SUSY Standard Model (MSSM) superpotential in order to incorporate R-parity violation (RPV):

$$W_{\not{R}_p} = \frac{1}{2}\lambda_{ijk}L_iL_j\bar{E}_k + \lambda'_{ijk}L_iQ_j\bar{D}_k + \frac{1}{2}\lambda''_{ijk}\bar{U}_i\bar{D}_j\bar{D}_k + \kappa_iL_iH_2\,, \qquad (1.1)$$

where gauge indices have been suppressed.

In the MSSM lagrangian, SM and SUSY particles are grouped together into lepton (L_i), quark (Q_i) and Higgs ($H_{1,2}$) SU(2) doublet superfields and electron (E_i), down (D_i) and up (U_i) SU(2) singlet superfields. In eq. (1.1), λ_{ijk}, λ'_{ijk} and λ''_{ijk} are Yukawa couplings between the matter superfields and κ_i is the mixing term between the lepton and Higgs doublets. The subscripts i, j and k are family indices. λ_{ijk} is antisymmetric under $i \leftrightarrow j$ and λ''_{ijk} is antisymmetric under $j \leftrightarrow k$. $W_{\not{R}_p}$ therefore adds $9 + 27 + 9 + 3 = 48$ free parameters to the MSSM superpotential.

Interactions involving the λ_{ijk}, λ'_{ijk} and κ_i couplings violate lepton number, while those involving the λ''_{ijk} coupling violate baryon number. The simultaneous presence of the second and third terms in eq. (1.1) can lead to fast proton decay in gross conflict with the lower limit on the proton lifetime [3]. Since both lepton and baryon number violation are required in order for the proton to decay, current experimental bounds on the proton lifetime and other SM processes can be respected if either baryon number or lepton number is conserved [2].

The difference in experimental signatures between RPV and RPC SUSY models at the LHC depends on the strength of the RPV coupling. We will concentrate on the trilinear couplings and neglect the bilinear term which leads to mixing between the leptons and gauginos, and between the sleptons and Higgs bosons. When the RPV couplings are small compared to the MSSM gauge couplings, the dominant effect is that the LSP can decay into SM particles. For example, the lifetime of the LSP ($\tilde{\chi}_1^0$) as a function of the RPV coupling λ''_{212} is shown in figure 1a.

If the RPV couplings and MSSM gauge couplings are of the same order of magnitude, RPV production processes and decays of particles heavier than the LSP become important. For a large λ''_{ijk} coupling, the branching fractions of RPC and RPV decays of a squark can be of the same order of magnitude (figure 1b), and SUSY particles can be produced singly, as was investigated in [4].

In the present analysis, λ''_{212} is the only RPV coupling set to a non-zero value. This gives rise to the LSP decay mode $\tilde{\chi}_1^0 \to cds$. This is the most challenging case experimentally, since there are no leptons or b-quarks among the $\tilde{\chi}_1^0$ decay products which can be used as tags for signal events. Unlike many other RPV couplings, λ''_{212} is not currently constrained by experiment [5]. The case of a non-zero coupling λ''_{112} is equally challenging but the limits on this coupling from heavy nucleon decay and neutron-antineutron oscillations are very strict [5]. However our analysis would also apply to this coupling if it is large enough to give an observable signal. As each event will usually contain two $\tilde{\chi}_1^0$'s there will be at least six jets in the final state.
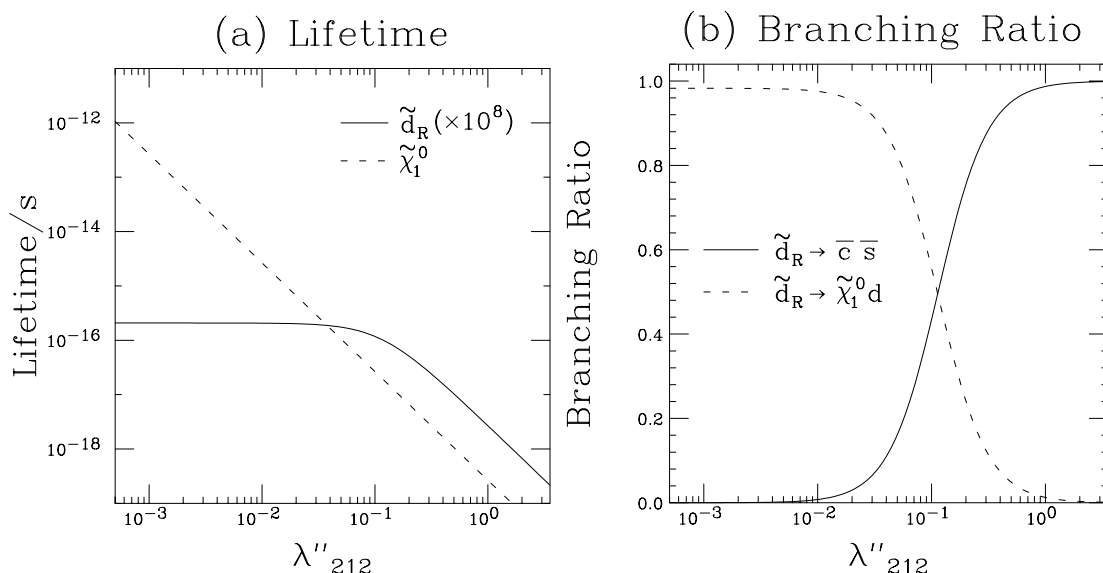
Figure 1: (*a*) Lifetimes of the $\tilde{d}_R$ and $\tilde{\chi}_1^0$ and (*b*) branching ratio of RPC (dashed) and RPV (solid) decays of the $\tilde{d}_R$, plotted against λ''_{212} at the SUGRA point $m_0 = 100\,\mathrm{GeV}$, $m_{1/2} = 300\,\mathrm{GeV}$, $A_0 = 300\,\mathrm{GeV}$, $\tan\beta = 10$ and sgn μ +.

$\tilde{\chi}_1^0$	$\tilde{\chi}_2^0$	$\tilde{g}$	$\tilde{u}_R$	$\tilde{u}_L$	$\tilde{d}_R$	$\tilde{d}_L$	$\tilde{l}_R$	$\tilde{l}_L$	h^0
116.7	211.9	706.3	611.7	632.6	610.6	637.5	155.3	230.5	112.7

Table 1: Masses of selected particles (GeV) for the model investigated.

The RPV coupling was added to a minimal supergravity (mSUGRA) model with 5 GUT-scale parameters: a universal scalar mass $m_0 = 100\,\mathrm{GeV}$, a universal gaugino mass $m_{1/2} = 300\,\mathrm{GeV}$, trilinear $H\tilde{f}\tilde{f}$ soft SUSY breaking terms $A_0 = 300\,\mathrm{GeV}$, the ratio of the vacuum expectation values of the two Higgs doublets $\tan\beta = 10$ and the sign of the SUSY higgsino mass parameter μ positive. It should be noted that we have only included the RPV coupling at the weak scale, i.e. the RPV coupling is not used in the evolution from the GUT scale, as was done in [6].

Five sets of parameter values have been extensively studied in the R_P conserving MSSM. The parameters chosen here correspond to SUGRA Point 5, with one modification: the value of $\tan\beta$ has been increased from 2.1 to 10 in order to keep the predicted Higgs mass above the current experimental limit. The masses of some key particles in this model are given in table 1. Searches in the SUGRA Point 5 scenario have been well studied in the case of a stable $\tilde{\chi}_1^0$ [1]. At this SUGRA point, the $\tilde{\chi}_1^0$ is the LSP, as must be the case for our analysis to be valid, even though cosmological constraints which require the LSP to be neutral only apply if it is stable.

The case of $\lambda''_{212} = 0.005$ is considered first. This coupling strength gives rise to decay chains essentially identical to those in an RPC model, except for the decay of the $\tilde{\chi}_1^0$ inside the beam pipe, with a lifetime of $1.0 \times 10^{-14}\,\mathrm{s}$.

The effect of varying the RPV coupling in our analysis will be discussed in section 6. For RPV couplings of order 10^{-6} or smaller [7], the LSP has a sufficiently

long lifetime to decay outside of the detector. If the LSP is charged, heavily ionizing low velocity tracks would be seen in the detector, providing a clear signature. This analysis addresses the case of a neutral LSP, the lightest neutralino ($\tilde{\chi}_1^0$), which has negligible interactions with the detector. For low RPV couplings, the experimental signature is then identical to that of an RPC model. However, if RPV couplings are above 10^{-4} [7], the LSP usually decays in the beam pipe and the missing energy signature, seen in RPC models, is not present.

2. Analysis strategy

In this work, HERWIG 6.1 [8] is used as the event generator,[1] and the official ATLAS simulation program ATLFAST [10] is used to simulate the performance of the ATLAS detector. Since each $\tilde{\chi}_1^0$ decays to three quarks, and in general the decay chain produces the $\tilde{\chi}_1^0$ in association with at least one other quark (typically from squark decay), the mean jet multiplicity (N_{jet}) in the signal events is high.

The principal difficulty in measuring the $\tilde{\chi}_1^0$ mass is the identification of the correct jets from the $\tilde{\chi}_1^0$ decay. Nearly all right-squarks decay via $\tilde{q}_R \to \tilde{\chi}_1^0 q \to qqqq$ and one might therefore expect $N_{\mathrm{jet}} = 8$ for $\tilde{q}_R\tilde{q}_R$ production. Gluon radiation by quarks, however, raises this to an average of 9.2 jets, in spite of the fact that the three jets from harder $\tilde{\chi}_1^0$s are spatially close together and some merging of jets occurs. In $\tilde{q}_L\tilde{q}_L$ events $N_{\mathrm{jet}} = 10.7$. The increase with respect to the right-handed states is due to the difference in couplings to charginos and neutralinos. Gluinos mostly decay into a squark and a quark and $\tilde{g}\tilde{g}$ events have a higher value of $N_{\mathrm{jet}} = 12.8$. A simple algorithm is used to calculate the jet energies, summing the energy within a cone of size 0.4 about the jet axis in the $\eta - \phi$ plane, and at least 8 jets with $E_T > 25\,\mathrm{GeV}$ are required in signal events.

The analysis proceeds in the following steps:

- Cuts are applied to reduce the SM background to below 10% of the SUSY signal. These cuts rely on the presence of lepton pairs in the signal events. Such lepton pairs are produced from the decay chain $\tilde{\chi}_2^0 \to \tilde{l}_R\, l \to ll\tilde{\chi}_1^0$ in most SUSY models. An analysis based on looking for events with two such $\tilde{\chi}_2^0$ decays was proposed in [11] but the rate for events with four leptons is much lower than for events with only one $\tilde{\chi}_2^0$ decay of this type.

- In each signal event, cuts are made on the jet transverse momenta (p_T) in order to preferentially select jets from neutralino decays.

- All possible combinations of three of the selected jets are inspected, and their invariant mass, m_{jjj}, calculated. Events are retained if two combinations are compatible with the same candidate $\tilde{\chi}_1^0$ mass.

---

[1]The simulation of RPV events in HERWIG is discussed in [9].

- One of these three-jet $\tilde{\chi}_1^0$ candidates is combined with an opposite sign, same flavour (OSSF) lepton pair. The invariant mass of this system, $m_{jj\ell\ell}$, is a $\tilde{\chi}_2^0$ candidate. A clear peak at the $\tilde{\chi}_1^0, \tilde{\chi}_2^0$ masses in the m_{jjj}, $m_{jj\ell\ell}$ plane is then observed.

- The $\tilde{l}_R$ and the $\tilde{q}_L$ masses are reconstructed using 3-jet combinations in the 2-dimensional $\tilde{\chi}_1^0, \tilde{\chi}_2^0$ mass peak.

In the following sections, each of these steps is considered in turn.

3. Standard model background

The SM background in this model is considered in [1]. It is shown in [12] that the inclusive SUSY signal can be separated from the SM background by requiring that each event contains:

- at least 8 jets with $E_T > 25\,\text{GeV}$;

- at least one jet with $E_T > 100\,\text{GeV}$;

- transverse sphericity > 0.2, transverse thrust < 0.9;

- $m_{T,\text{cent}} > 1\,\text{TeV}$, where $m_{T,\text{cent}} = \sum p_T^{\text{jet}} + \sum p_T^{\text{lepton}}$, where the sum includes central jets and leptons (i.e. with pseudorapidity $|\eta| < 2$);

- at least two leptons (e or μ) with $p_T > 15\,\text{GeV}$ and $|\eta| < 2.5$.

With these cuts, the signal to background ratio is greater than 10. The SM background has not been explicitly simulated in this study. Current Monte Carlo event generators are not capable of reliably simulating QCD eight jet plus two lepton production. We have therefore simulated eight jets and two leptons distributed according to phase space.

In SUSY events, lepton pairs are created in the decay $\tilde{\chi}_2^0 \rightarrow \tilde{l}_R l \rightarrow ll\tilde{\chi}_1^0$. The leptons are therefore required to have opposite charges and the same flavour (OSSF). The invariant-mass distribution of the lepton pairs created in this decay has a kinematic edge [1, 13] which is given by

$$m_{\ell\ell}^{\max} = \sqrt{\frac{[m^2(\tilde{\chi}_2^0) - m^2(\tilde{l}_R)] \times [m^2(\tilde{l}_R) - m^2(\tilde{\chi}_1^0)]}{m^2(\tilde{l}_R)}}, \qquad (3.1)$$

and is simulated after experimental resolution in figure 2.

With the particular parameter set chosen this edge is calculated as 95.1 GeV. Accordingly, events are required to have a lepton pair with an invariant mass below this value. The corresponding edge can be easily measured for other parameter sets.
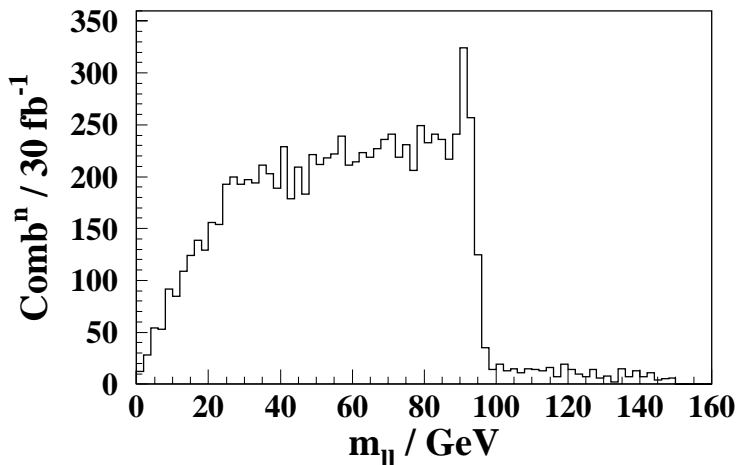
Figure 2: The dilepton invariant mass for events with an OSSF electron or muon pair, after the SM cuts have been applied. The kinematic limit for the decay chain shown in figure 3 is at $95.1\,\text{GeV}$. Events are excluded if there is no jet combination which passes the jet cuts described in section 4. For the SUGRA point chosen it happens that the kinematic edge lies just above the peak at $m(\text{Z}^0)$ from the decay $\text{Z}^0 \to \ell\ell$.
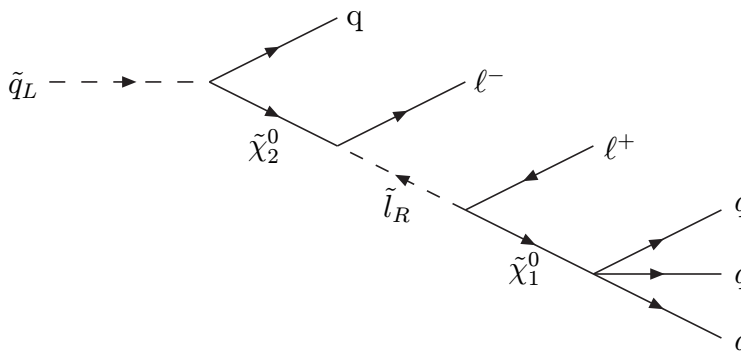

Figure 3: One of the decay chains of the $\tilde{q}_L$ contributing to the signal.

4. Detection of the $\tilde{\chi}_1^0$ and $\tilde{\chi}_2^0$

Many different decay chains can contribute to the SUSY signal selected by the cuts. One important example, $\tilde{q}_L \to \tilde{\chi}_2^0 q \to \tilde{l}_R l q \to \tilde{\chi}_1^0 l l q \to qqqllq$, is shown in figure 3.

When λ''_{212} is small, there are nearly always two $\tilde{\chi}_1^0$s produced in an event and one can therefore search for two sets of three jets with similar invariant mass. An upper limit on the invariant mass difference of $\delta m_{jjj} = |m_{jjj}^{(a)} - m_{jjj}^{(b)}| < 20\,\text{GeV}$ is used in this analysis, where a and b label the two $\tilde{\chi}_1^0$ LSP candidates.

In order to limit the combinatorial background, the search for the $\tilde{\chi}_1^0$ signal is initially restricted to events with $8 \leq N_{\text{jet}} \leq 10$, with the following cuts on the
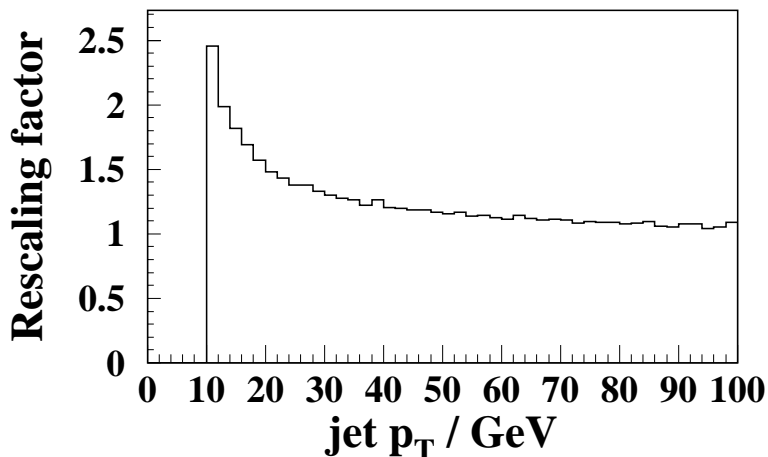
Figure 4: The rescaling factor applied to the observed jet energy as a function of jet p_T.

allowed range of jet transverse momenta in GeV:

- $100 < p_T^{(a1)}$; $17.5 < p_T^{(a2)} < 300$; $15.0 < p_T^{(a3)} < 150$;

- $17.5 < p_T^{(b1)} < 300$; $17.5 < p_T^{(b2)} < 150$; $15.0 < p_T^{(b3)} < 75$,

where $a1$ denotes the highest p_T jet from neutralino candidate a, etc.

Candidate sets of jets from the $\tilde{\chi}_1^0$ decay can also be identified by their separation in the $\eta - \phi$ plane. For both $\tilde{\chi}_1^0$s, cuts are made on the distance between the hardest and next hardest jets (ΔR_{12}) and between the combined momentum vector of the two hardest quarks and the softest quark (ΔR_{12-3}). The following cuts are chosen based on simulations:

- $\Delta R_{12}^{(a)} < 1.3$; $\Delta R_{12-3}^{(a)} < 1.3$;

- $\Delta R_{12}^{(b)} < 2.0$.

Since the SUSY cross section is dominated by production of squarks and gluinos, about 95% of events have two hard jets with $E_T^{(h1)} > 200\,\mathrm{GeV}$ and $E_T^{(h2)} > 100\,\mathrm{GeV}$ from the squark decays. We require that two jets in an event satisfy these cuts. We do not use those two jets to construct $\tilde{\chi}_1^0$ candidates. This decreases the background from wrong combinations.

For each combination of jets passing the kinematic cuts, the jet energies are rescaled according to their p_T, to allow for energy lost out of the jet cones. The rescaling function, shown in figure 4, is the ratio p_T^{jet}/p_T^u used in ATLFAST.

The reconstructed masses of all $\tilde{\chi}_1^0$ candidates are included in figure 5. If two or more combinations of jets from one event pass the cuts, the masses from each combination are plotted with unit weight. However this can lead to one event contributing a large number of combinations and therefore if there are more than five
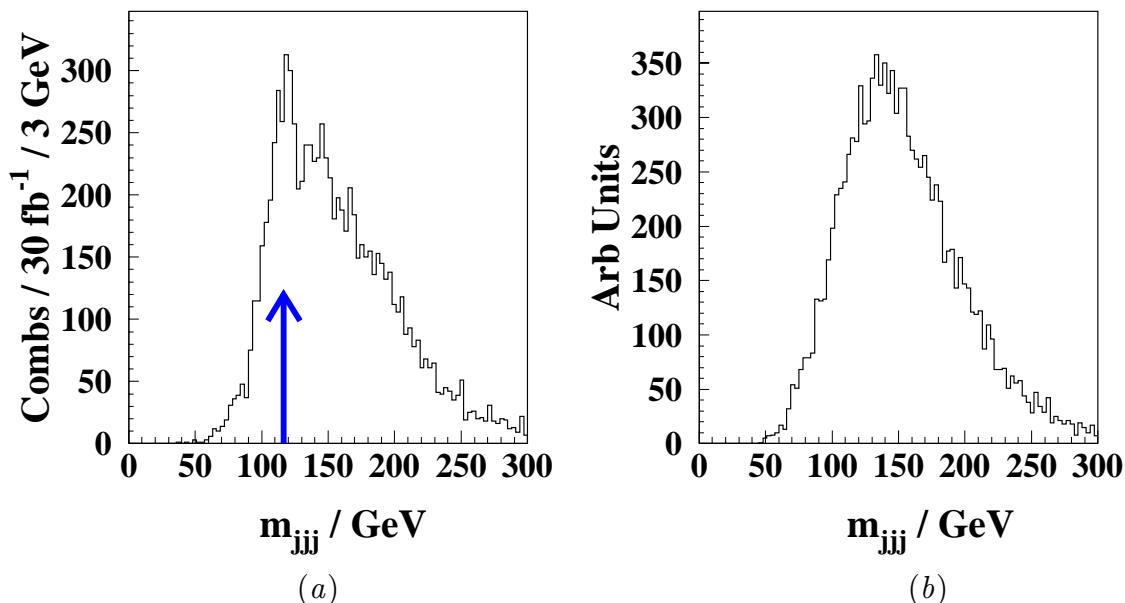
Figure 5: (a) The invariant mass of three-jet combinations passing the cuts described in the text. The mass peak from the decay $\tilde{\chi}_1^0 \to qqq$ can be seen above the background from wrong combinations of jets. The input $\tilde{\chi}_1^0$ mass is indicated by the arrow. (b) A phase-space sample shows a peak in much the same region.

combinations which pass the cuts only the five with the smallest difference between the $\tilde{\chi}_1^0$ candidate masses are included.

In events with more than one combination passing the cuts, two combinations of jets often differ only in the choice of jets for one of the two $\tilde{\chi}_1^0$s. In such cases, the unique mass combination is included in the histogram only once. The two ambiguous masses are both included with unit weight.

There is a broad combinatorial background beneath the $\tilde{\chi}_1^0$ mass peak in figure 5a, the shape of which is defined by the kinematic cuts and is reproduced by the phase-space sample, as shown in figure 5b. In order to further suppress the background we attempt to find the mass of the $\tilde{\chi}_2^0$ in the decay chain $\tilde{\chi}_2^0 \to \tilde{l}_R l \to ll\tilde{\chi}_1^0$ by forming the total invariant mass of the OSSF dilepton pair and one of the 3-jet candidates. We choose the $\tilde{\chi}_1^0$ candidate which is nearest in $\eta - \phi$ to either lepton.

By using the extra information from the leptons we are able to supress the combinatorial background. A clear peak in the $(\tilde{\chi}_1^0, \tilde{\chi}_2^0)$ mass plane is visible in figure 6a. Figure 7 shows slices through the peak along the axes $m^{\pm} = (m_{jjj} \pm m_{jj\ell\ell})/\sqrt{2}$. The peak is present in the central slices, while the sidebands show similar shapes to the background under the peak. It is clear that this peak is not determined by the kinematic cuts, as it is absent in our phase-space sample (figure 6b). In addition we find that the position of the peak accurately follows the input masses, when those are varied from (116.7, 211.9) to (137.8, 252.6) GeV.

The data in the rectangle shown in figure 6 were fitted with a 2-d gaussian. Since m_{jjj} and $m_{jjj\ell\ell}$ are highly correlated, the peak was fitted in the rotated (m^+, m^-)
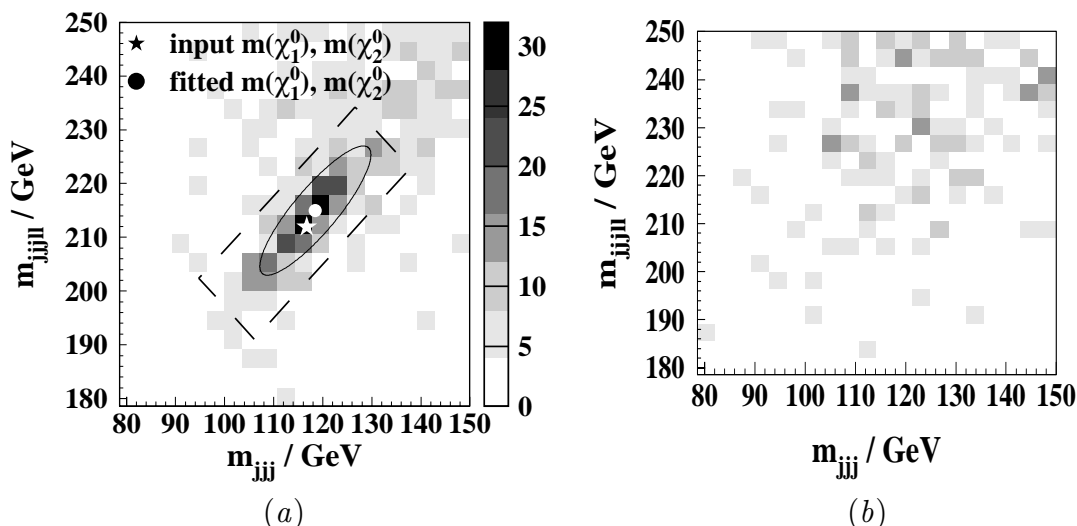
Figure 6: (a) The $\tilde{\chi}_1^0$ (m_{jjj}) and $\tilde{\chi}_2^0$ ($m_{jjj\ell\ell}$) candidates. The number of jet combinations passing the cuts per $30\,\mathrm{fb}^{-1}$ is given by the key. The circle and the ellipse show the peak and standard deviation of a 2-d gaussian fitted to the data contained in the dashed box. The star shows the input masses. (b) The corresponding $(m_{jjj}, m_{jjj\ell\ell})$ invariant mass combinations from the phase-space sample show no such peak.
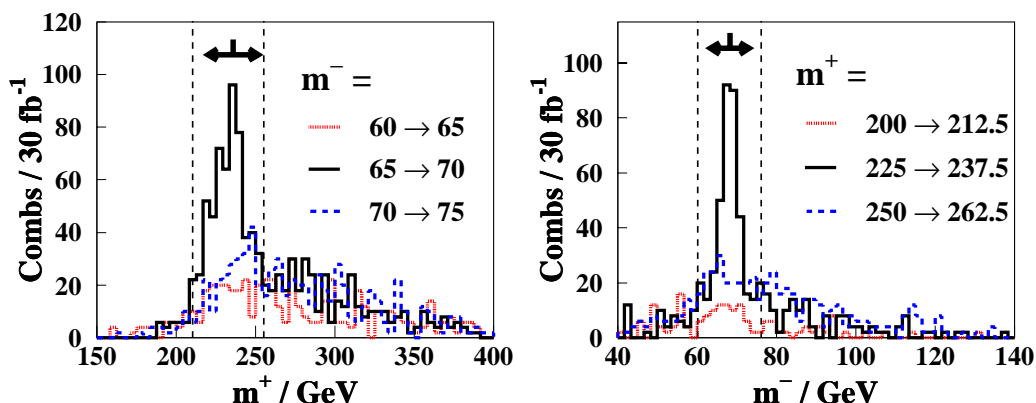

Figure 7: Slices taken through figure 6a in the rotated (m^+, m^-) coordinate directions. The fit was performed on the data contained in the region between the dotted lines. The fitted peak and width are given by the thick line and arrow at the top of each plot.

coordinate system in which the correlations are smaller. The mass difference relies on lepton rather than jet momenta, so the width in the m^- direction (4 GeV) is smaller than in the m^+ direction (15 GeV). The standard error on the peak was 4.5 GeV in m^- and 1.5 GeV in m^+. This corresponds to a 3 GeV uncertainty in each of the neutralino masses.

Our fitted masses, at $m(\tilde{\chi}_1^0, \tilde{\chi}_2^0) = (118.9, 215.5)$ GeV are slightly high when compared to the input values of $(116.7, 211.9)$. This is due to several effects, including overlap between the jets, and the contribution of energy from the underlying event in the jet cones. Indeed we would expect that our simple rescaling factor will over-
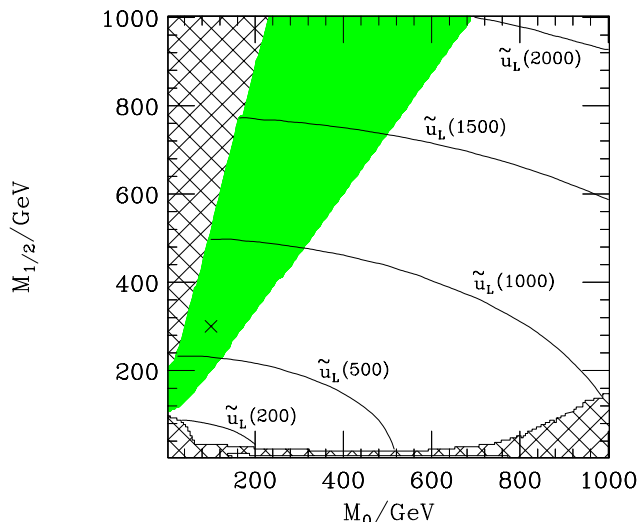
Figure 8: The region of mSUGRA parameter space over which the decay $\tilde{\chi}_2^0 \to \tilde{l}_R \ell \to \tilde{\chi}_1^0 \ell\ell$ occurs is shaded. M_0 is the universal scalar mass, and $M_{1/2}$ is the universal gaugino mass at the GUT scale. The lower hatched region is excluded by incorrect symmetry breaking minima, whereas in the the upper hatched region the $\tilde{\chi}_1^0$ is not the LSP and our analysis does not apply. The contours show the mass of the $\tilde{u}_L$ squark. The $\times$ marker shows the chosen point. The other parameters are: $\tan\beta = 10$, $A_0 = 300\,\text{GeV}$ and $\text{sgn}(\mu) = +$.

compensate for energy losses from jet cones, since the three jets from the $\tilde{\chi}_1^0$ decay are close in $\eta - \phi$, so energy losses from one cone can end up in one of the other two.

A fuller investigation of these effects is beyond the scope of this study, requiring as it does a full investigation of the calorimeter calibration procedure for multi-jet events. It is estimated that in the actual experiment, the uncertainty in the absolute jet energy scale will be of the order of 1% for jets with $p_T > 50\,\text{GeV}$ [1]. For lower energy jets an uncertainty of 2–3% is more likely. With real data, therefore, it may be possible to reduce the systematic uncertainty on the $\tilde{\chi}_1^0$ mass to $3\,\text{GeV}$.

5. Detection of the $\tilde{l}_R$ and $\tilde{q}_L$

For the measurement of the slepton mass, having fitted the $\tilde{\chi}_1^0$ and $\tilde{\chi}_2^0$ masses, we select combinations within $1 \times \sigma$ of the peak. These combinations, with two OSSF leptons preferentially select the decay chains $\tilde{\chi}_2^0 \to \tilde{l}_R l \to ll\tilde{\chi}_1^0$, and $\tilde{\chi}_2^0 \to Z^0\tilde{\chi}_1^0$. Only the former can be used for $\tilde{l}_R$ measurements. The region of mSUGRA parameter space in which this chain will exist is given by the condition $m(\tilde{\chi}_2^0) > m(\tilde{l}_R)$, and is shown in figure 8.

The dilepton invariant mass distribution, figure 2, for our point in MSSM parameter space shows only a very small peak at the Z^0 mass, but a clear kinematic edge, indicating that the slepton decay chain $\tilde{\chi}_2^0 \to \tilde{l}_R l \to ll\tilde{\chi}_1^0$ dominates. This is
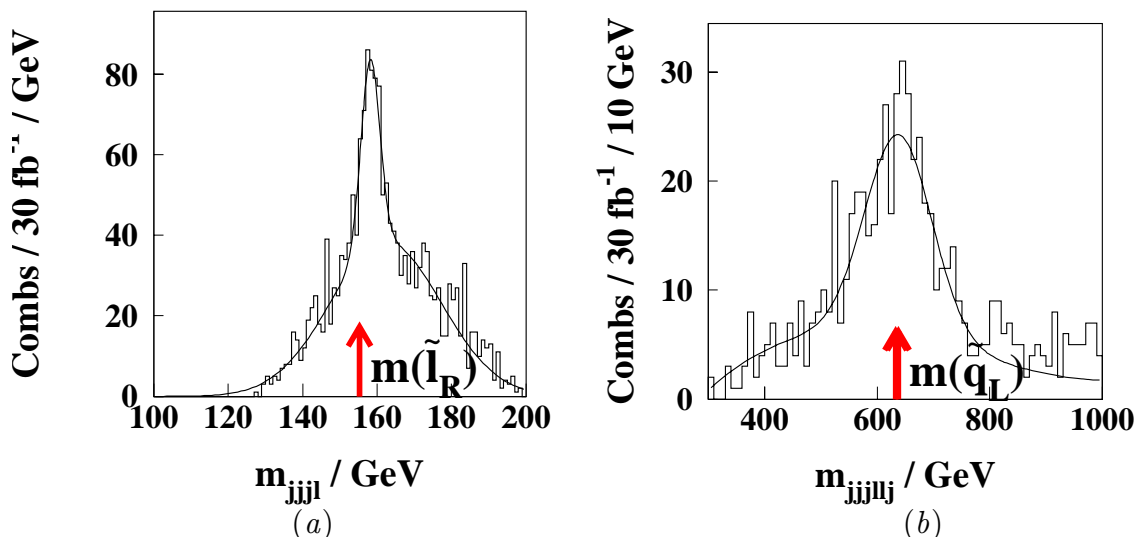
Figure 9: The masses of (a) $\tilde{l}_R$ and (b) $\tilde{q}_L$ candidates. Only combinations from under the $(\tilde{\chi}_1^0, \tilde{\chi}_2^0)$ mass peak, and satisfying the cuts described in the text are plotted. Each jjj invariant mass has been rescaled to the fitted $\tilde{\chi}_1^0$ mass. The $\tilde{l}_R$ and $\tilde{q}_L$ masses are indicated by the arrows. The fitted functions are described in the text.

expected at this point, since the $m(\tilde{\chi}_2^0) - m(\tilde{\chi}_1^0)$ mass difference of $95.2\,\text{GeV}$ means that there is little phase space available for the decay $\tilde{\chi}_2^0 \to Z^0 \tilde{\chi}_1^0$. If the masses and couplings for this decay were significant, then we would exclude events with dilepton invariant mass near $m(Z^0)$ from the $\tilde{l}_R$ measurement. Both chains may have been preceded by $\tilde{q}_L \to \tilde{\chi}_2^0 q$, so both can be used for the $\tilde{q}_L$ mass measurement.

We recall that the initial sample of $\tilde{\chi}_1^0$ candidates was restricted to events with $8 \leq N_{\text{jet}} \leq 10$ in order to reduce the combinatoric background. However, choosing combinations from under the $(\tilde{\chi}_1^0, \tilde{\chi}_2^0)$ mass peak removes much of the background, so in this section the jet multiplicity cut is therefore relaxed to $8 \leq N_{\text{jet}} \leq 11$ in order to increase the statistics. The invariant mass of the three-jet neutralino candidates is adjusted to the best-fit mass of the $\tilde{\chi}_1^0$, by rescaling the $\tilde{\chi}_1^0$ jet momenta by the same factor.

The $\tilde{l}_R$ mass is found by combining the $\tilde{\chi}_1^0$ candidate closest to a lepton in $\eta - \phi$ with that lepton. The resulting invariant mass distribution, m_{jjjl}, is shown in figure 9a. The sharp peak was fitted with a gaussian, with another gaussian for the background. This gave $m(\tilde{l}_R) = 157.8 \pm 0.3\,\text{GeV}$, which is slightly high when compared to the input value of $155.3\,\text{GeV}$ for the same reasons as were discussed in section 4.

The experimental electron and muon momentum scale uncertainties are expected to be small fractions of 1% [1], so the systematic error in the slepton mass measurement will be dominated by the same ($3\,\text{GeV}$) jet scale uncertainty as $m(\tilde{\chi}_1^0)$. The statistical error in rescaling the 3-jet invariant mass to the fitted $m(\tilde{\chi}_1^0)$ peak introduces another $3\,\text{GeV}$ systematic error into the $\tilde{l}_R$ and $\tilde{q}_R$ masses. The overall systematic error in $m(\tilde{l}_R)$ is therefore $3 \oplus 3 = 4.2\,\text{GeV}$.

The hardest two jets in the event are assumed to have come from squark or gluino decay, and so are not used in making three-jet combinations for neutralino candidates. The $\tilde{q}_L$ mass is found by combining each $\tilde{\chi}_2^0$ candidate with the harder of these two leading jets. To reduce the background we select combinations within $2 \times \sigma$ of the m($\tilde{l}_R$) peak. This allows us to relax the cut about the ($\tilde{\chi}_1^0, \tilde{\chi}_2^0$) peak from 1 to $2 \times \sigma$. The resultant invariant mass distribution, $m_{jj\ell\ell j}$, is shown in figure 9b. A peak is visible near the $\tilde{u}_L$ and $\tilde{d}_L$ masses of 633 GeV and 638 GeV, respectively, but the resolution is not sufficient to separate the states.

The background was modelled by finding the invariant-mass distribution of the $\tilde{\chi}_2^0$ candidates with the hardest jet from other $\tilde{q}_L$ candidate events. A gaussian fit to the signal with this background shape gave $m(\tilde{q}_L) = 637 \pm 5$ GeV. The uncertainty in modelling the background was estimated by fitting the distribution with other, simpler background shapes. These decrease position of the peak to 634 GeV (for a resonance-shaped background) to 627 GeV (for a linear background). This shows a systematic uncertainty in the $\tilde{q}_L$ mass of about 10 GeV. The hard jet used in the calculation of $m(\tilde{q}_L)$, has $p_T > 100$ GeV introducing an uncertainty in the mass scale of 1% [1], or 6 GeV. Carrying forward a 3 GeV uncertainty in the jjj invariant mass scale and 3 GeV from the $\tilde{\chi}_1^0$ fit, the total systematic error in the squark mass is 12 GeV.

At this SUGRA point the dominant decay mode of the $\tilde{q}_R$ is $\tilde{q}_R \to \tilde{\chi}_1^0 q$. One might therefore try to reconstruct the $\tilde{q}_R$ mass by combining the $\tilde{\chi}_1^0$ candidate not used in the $\tilde{q}_L$ reconstruction with the second hard jet. However while the cuts we applied to reduce the Standard Model background, i.e. requiring the presence of two leptons, mean that all the signal events contain a $\tilde{q}_L$, they do not necessarily contain a right squark. Only a third of the signal events actually contain a $\tilde{q}_R$. Most of the SUSY events at this SUGRA point come from gluino production which will either be rejected due to the large number of jets or contain additional hard jets from the gluino decay, and hence have a large combinatoric background for the $\tilde{q}_R$ reconstruction. In an attempt to reduce this background it is possible to use cuts on the $\tilde{\chi}_2^0$ and $\tilde{l}_R$ masses from $\tilde{q}_L$ decay on the other side of the event such that there is only one $\tilde{q}_R$ candidate. However this reduces the statistics so that a signal cannot be observed. This combination of factors makes it impossible to reconstruct the $\tilde{q}_R$ mass at this SUGRA point with the available statistics.

6. Other values of λ''_{212}

The method outlined above is relatively insensitive to the size of the coupling λ''_{212}. However as the RPV coupling λ''_{212} is decreased, the lifetime of the $\tilde{\chi}_1^0$ increases as shown in figure 1a. The method will start to fail when $\tilde{\chi}_1^0$s predominately decay beyond the first tracking layer of the detector. Special reconstruction could increase this by about an order of magnitude, at which point the decays would occur out-
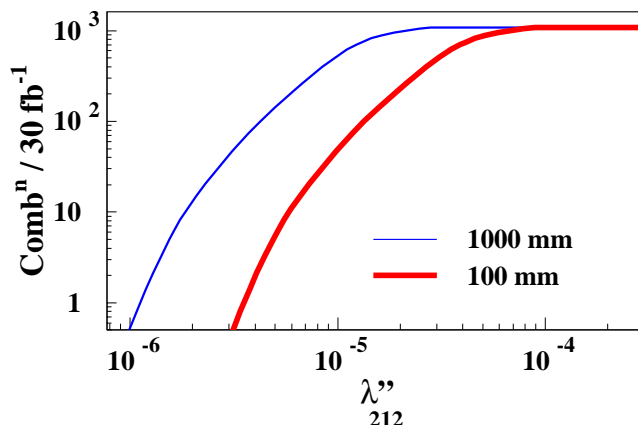
Figure 10: The number of jet combinations with transverse decay lengths less than 100 mm (thick line), and less than 1000 mm (thin line), as a function of the RPV coupling. Combinations beyond $1 \times \sigma$ of the $(\tilde{\chi}_1^0, \tilde{\chi}_2^0)$ peak found for $\lambda''_{212} = 0.005$ are excluded.

side of the tracking volume. We therefore exclude events when one or other of the $\tilde{\chi}_1^0$s has travelled more than 100 mm (1000 mm) from the interaction point in the transverse direction.

As can be seen in figure 10 statistics become limiting for λ''_{212} less than about 10^{-5}, when $c\tau \approx 800$ mm. With smaller couplings the RPV decay of the $\tilde{\chi}_1^0$ effectively switches off, and a RPC analysis based on a missing transverse energy + lepton(s) signature, such as [13], is effective.

If λ''_{212} is larger than 0.1, an initial $\tilde{q}_R$ often decays immediately into 2 jets and then only one 3 jet invariant mass combination will necessarily be close to the neutralino mass.

The size of the RPV coupling can be determined from the $\tilde{\chi}_1^0$ lifetime, as shown in figure 1a. The lifetime is, in principle, measurable for a wide range of couplings, by using vertexing information. However the need for detector-level Monte-Carlo simulation makes the measurement of λ''_{212} beyond the scope of this paper.

7. Conclusions

The usual ubiquitous signature for the R_P conserving MSSM is missing transverse energy. This signature disappears once R_P violating couplings are added, unless they are extremely small and the lifetime of a neutralino LSP is such that it decays outside the detector.

We examined the case where the neutralino LSP is unstable and decays to 3 jets with no particular tags on them (for example b's). This corresponds to the RPV coupling λ''_{212}, the trilinear RPV coupling giving the hardest case in which to detect and measure sparticles.

By analysing the decay chain, $\tilde{q}_L \to \tilde{\chi}_2^0 q \to \tilde{l}_R \ell q \to \tilde{\chi}_1^0 \ell\ell q$, we have shown that the $\tilde{\chi}_1^0$, $\tilde{\chi}_2^0$ and $\tilde{q}_L$ be detected and their masses measured, and that the mass of the $\tilde{l}_R$ can also be obtained in much of parameter space. The sparticle production and decays in this signal are all R_P conserving apart from the $\tilde{\chi}_1^0$ decay into 3 jets.

Although we have used a point near SUGRA Point 5 to derive the soft SUSY breaking parameters, the method should in principle work for other more general SUSY breaking parameter sets in which the decay chain in figure 3 exists. When some of the sparticles involved in the decay chain become much heavier than $1\,\mathrm{TeV}$, the analysis will become statistics limited.

To summarise, in the MSSM with a trilinear RPV coupling, even in the hardest choice of λ_{212}'', it is possible to detect sparticles and measure their masses at the LHC.

Acknowledgments

References

[1] ATLAS collaboration, *ATLAS detector and physics peformance TDR*, Technical Report CERN/LHCC 99-15, CERN, (1999) and the refereneces therein.

[2] H. Dreiner, *An introduction to explicit R-parity violation*, in *Perspectives on super-symmetry*, G.L. Kane ed., World Scientific, 1997 [hep-ph/9707435];
G. Bhattacharyya, *A brief review of R-parity-violating couplings*, hep-ph/9709395.

[3] Particle Data Group *Review of particle physics*, *Eur. Phys. J.* **C 15** (2000) 1.

[4] P. Chiappetta, A. Deandrea, E. Nagy, S. Negroni, G. Polesello and J.M. Virey, *Single top production at the LHC as a probe of R-parity violation*, *Phys. Rev.* **D 61** (2000) 115008 [hep-ph/9910483];
B. Allanach et al., *Searching for R-parity violation at Run-II of the Tevatron*, hep-ph/9906224;
S. Dimopoloulos et al., *Cross-sections for lepton and baryon number violation processes from supersymmetry at $p\bar{p}$ colliders*, *Phys. Rev.* **D 41** (1990) 2099;
J.-M. Yang et al., *Top quark at the upgraded Tevatron to probe new physics*, hep-ph/9802305;
A. Dalta et al., *Effects of R-parity-violating supersymmetry in single top production at the Tevatron*, *Phys. Rev.* **D 56** (1997) 3107;
R.J. Oakes, K. Whisnant, J.M. Yang, B.-L. Young and X. Zhang, *Single top quark production as a probe of R-parity-violating susy at $p\ p$ and $p\bar{p}$ colliders*, *Phys. Rev.* **D 57** (1998) 534 [hep-ph/9707477];

E.L. Berger, B.W. Harris and Z. Sullivan, *Direct probes of R-parity-violating super-symmetric couplings via single-top-squark production*, `hep-ph/0012184`;

E.L. Berger, B.W. Harris and Z. Sullivan, *Single-top-squark production via R-parity-violating supersymmetric couplings in hadron collisions*, *Phys. Rev. Lett.* **83** (1999) 4472 [`hep-ph/9903549`].

[5] B.C. Allanach, A. Dedes and H.K. Dreiner, *Bounds on R-parity violating couplings at the weak scale and at the GUT scale*, *Phys. Rev.* **D 60** (1999) 075014 [`hep-ph/9906209`].

[6] B.C. Allanach, A. Dedes and H.K. Dreiner, *2-loop supersymmetric renormalisation group equations including R-parity violation and aspects of unification*, *Phys. Rev.* **D 60** (1999) 056002 [`hep-ph/9902251`].

[7] A. Mirea and E. Nagy, *Study of the determination of the SUGRA parameters using the ATLAS detector in the case of L-violating R parity breaking*, Internal ATLAS note PHYS-99-007, CERN, 1999 `hep-ph/9904354`.

[8] G. Corcella et al., HERWIG 6.1 *release note*, `hep-ph/9912396`;

HERWIG 6*: an event generator for hadron emission reactions with interfering gluons (including supersymmetric processes)*, *J. High Energy Phys.* **01** (2001) 010 [`hep-ph/0011363`];

G. Marchesini et al., HERWIG*: a Monte Carlo event generator for simulating hadron emission reactions with interfering gluons*, *Comput. Phys. Commun.* **67** (1992) 465.

[9] H. Dreiner, P. Richardson and M.H. Seymour, *Parton-shower simulations of R-parity violating supersymmetric models*, *J. High Energy Phys.* **04** (2000) 008 [`hep-ph/9912407`];

P. Richardson, *Simulations of R-parity violating SUSY models*, `hep-ph/0101105`.

[10] E. Richter-Was, D. Froidevaux and L. Poggioli, *ATLFAST 2.0: a fast simulation package for ATLAS*, Tech. Rep. ATL-PHYS-98-131, 1998.

[11] P. Binetruy et al., in *Proceedings, Large Hadron Collider*, vol. 2, 666-675 CERN-90-10-B, CERN, 1990.

[12] J. Soderqvist, *Consequences of baryonic R-parity violation for measurements of SUSY particles using the ATLAS detector*, Internal ATLAS note PHYS-98-122, CERN, 1998.

[13] B.C. Allanach, C.G. Lester, M.A. Parker and B.R. Webber, *Measuring sparticle masses in non-universal string inspired models at the LHC*, *J. High Energy Phys.* **09** (2000) 004 [`hep-ph/0007009`].